Voltage Distortion Minimization in Cascaded H-Bridge Inverters

António Martins[1(✉)], João Faria[1], and Abel Ferreira[2]

[1] Faculty of Engineering, University of Porto, Porto, Portugal
ajm@fe.up.pt, jpc.faria@hotmail.com
[2] CINERGIA - Control Intelligent de l'Energia, Barcelona, Spain
abel.ferreira@cinergia.coop

Abstract. Multilevel inverters based on the series connection of H-bridges are the most modular multilevel inverter family. The use of a large number of these devices connected in series, controlled by modulation based on the fundamental frequency, allows to obtain an output voltage of the inverter with low harmonic distortion and low losses in the inverter. This paper analyses the main characteristics of a fundamental frequency modulation method applied to multilevel inverters based on cascaded H-bridges (CHB). Particular emphasis is given to the harmonic distortion of the output voltage and the range of variation of the amplitude of the fundamental component in static and dynamic conditions. It is also discussed the implementation of the algorithm in real-time and in an FPGA platform. Simulation and experimental results are presented with a different number of H-bridges.

Keywords: Cascaded H-bridge inverters · Multilevel inverters · Square-wave modulation · Total harmonic distortion

1 Introduction

Multilevel inverters are electronic power converters that output a voltage wave with more than two levels. This waveform is more similar to a sine wave than that generated by a conventional two-level converter, thus presenting a lower total harmonic distortion. As with any other type of DC/AC converter, the control of the semiconductors is the means to control the output voltage, either via modulation index, number of bridges in series or contribution to the total fundamental component of each individual bridge. In relation to conventional topologies, the different multilevel topologies allow to reduce some additional less desirable properties that characterize them such as the reduction of switching and conduction losses, use of semiconductors of lower controlled power, reduction of voltage gradients, reduction of common mode voltages as well as overall reduction of electromagnetic interference. Therefore, input and/or output filters can be reduced or even eliminated, contributing to the increase of energy efficiency, [1,2].

J. L. Afonso et al. (Eds.): GreeNets 2018, LNICST 269, pp. 86–102, 2019.
https://doi.org/10.1007/978-3-030-12950-7_8

The multilevel converter architectures have some specific properties that should be emphasized: an increase in the number of controlled semiconductors, diodes and capacitors, the need for more elaborate semiconductor control and selection algorithms. In any of the architectures (conventional or multilevel), the harmonic content of the output voltage is reduced by increasing the switching frequency; however, either the specific technology of the semiconductors or the increase in switching losses limits that degree of freedom. The fundamental concept of the multilevel structure allowed the development of quite distinct topological alternatives with different expressions in the market, [1].

In this context, there are three main topologies of multilevel converters: with diode-clamped voltages, intermediate voltages defined by floating capacitors and single-phase bridges in series. In recent years, the MMC (modular multilevel converter) based on half-bridge or full-bridge has emerged, mainly with applications in the field of power conditioning in electric power grids and in medium and high power systems. In any configuration, single-phase and three-phase solutions are available in the market.

This work studies the configuration based on the series connection of full single-phase bridges and their single-phase topology. As mentioned above, the topology is modular and is applicable in medium and high power situations, being able to control very high voltages and able to define waveforms with very low total harmonic distortion (THD). This low value is possible since the total output voltage is obtained from the sum of many individual low-amplitude voltages with quasi-square waveform, i.e. switching at fundamental frequency thus maintaining very low switching losses, [2].

This paper is organized as follows: Sect. 2 describes and analyzes modulation methods, both high frequency (pulse width modulation) and fundamental frequency, for inverters in series. In the same section, two command methods are also analyzed at fundamental frequency with respect to the specific objectives and their ease of implementation in real-time, and one of them is selected for demonstration. The following Sect. 3 shows simulation results and characterizes the output voltage waveform (low frequency harmonics and total harmonic distortion). Section 4 presents experimental results for two inverters: with three single-phase inverters in series and with five inverters and discusses the main properties of the control method for a larger number of inverters. Finally, Sect. 5 discusses the main conclusions of the study.

2 Cascaded H-Bridge Inverters

A multilevel inverter with bridges in series consists of several inverters (H-bridges), as shown in Fig. 1 for the three-phase topology. Each elementary inverter is powered by an isolated source (or a capacitor) and can set three voltage levels ($-E$, 0 and $+E$) in the output. Thus, in order to obtain a greater number of levels in the overall output, more than one inverter is required to be connected in series provided that their individual voltages are not instantaneously equal. Thus, the resulting voltage may be more similar to a sine wave.

If the voltage values of the different sources are equal and if S is the number of bridges, the number of output voltage levels, N_L, is given by (1):

$$N_L = 2S + 1 \tag{1}$$

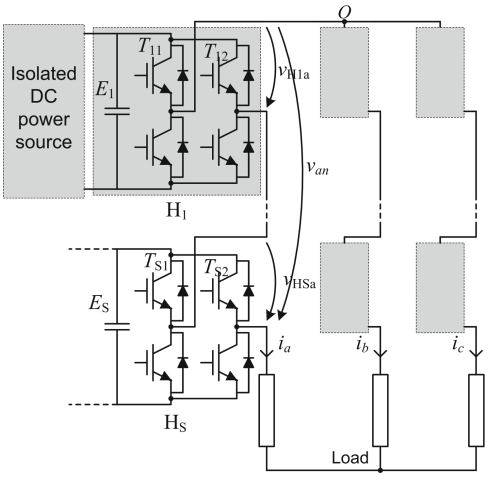

Fig. 1. Structure of a three-phase inverter based on series connection of single-phase full bridges.

If the inverters are fed by voltage sources of different value, a greater number of levels can be obtained in the global output, [1]. For two inverters, if the DC voltage values are, for example, $E_1 = E$ and $E_2 = 3E$, a 9-level waveform instead of 5 is obtained (when using the most common $E_1 = E_2 = E$). In principle, a high number of levels would produce a better waveform quality (i.e. a smaller THD) but, as will be demonstrated later, some important drawbacks occur in certain applications. Additionally, the semiconductors ($T_{1k}, T_{2k}, \ldots T_{Sk}$) are different and must be designed accordingly, therefore reducing the modularity of this converter.

The power structure of the inverter with cascaded bridges powered by regulated active power sources has several advantages and some specific aspects that must be considered within its application, [2]:

- Unlike other multilevel topologies, does not require balancing of DC voltages that feed the individual inverter
- Does not add diodes or capacitors to set the voltage levels
- Presents high modularity and is easily scalable in voltage and power.

The least favourable aspects identified in this topology are:

- It requires independent voltage sources for each bridge, which restricts the scope of its application
- Synchronous switching is required on bidirectional AC/DC/AC systems in order to avoid short circuits between isolated sources.

2.1 High-Frequency PWM

One of the main components of power losses in an inverter is the switching losses in the semiconductors which makes the switching frequency an important variable in the design; its impact should be considered and evaluated when it comes to defining the switching and modulation method.

For multilevel inverters, PWM-based switching methods are a generalization of the principle of operation for two-level inverters; multi-carrier PWM, [1,3]. For single-phase systems, PWM with level shift (LS-PWM) and PWM with phase shift (PS-PWM) can be used. However, the PS-PWM has a lower harmonic content, [3,4]. These methods have very good waveform quality (low THD of the voltage) and high bandwidth, which makes them preferable for low and medium power applications and high dynamic range. On the other hand, in high power applications, where switching losses are to be kept low, the fundamental frequency switching methods have specific advantages.

2.2 Low-Frequency Modulation Methods

Low-frequency modulation methods can be used in inverters with series bridges because of their specific configuration, [1]. In Fig. 2 the principle of operation of these methods is shown for an inverter with eleven levels (five bridges), where θ_k is the switching angle of the inverter k and E is the value of the DC voltage, common to all inverters.

The fundamental frequency modulation, or square wave modulation, is implemented to satisfy one of the possible objectives, [5–8]:

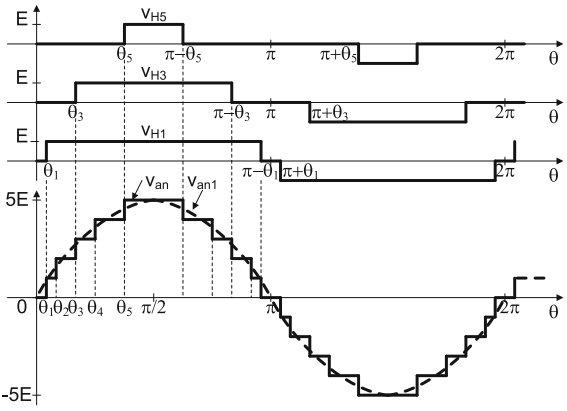

Fig. 2. Square-wave modulation: output voltage of three bridges and total output voltage when using five bridges.

- Minimizing the THD of the inverter output voltage
- Elimination of the main low-frequency harmonics of the output voltage, e.g. third, fifth, seventh, ...
- THD minimization of the output voltage of the inverter in three-phase systems (do not account for multiples of three)
- Elimination of the main low-frequency harmonics of the output voltage in three-phase systems, e.g. fifth, seventh, ...

As a first goal, in any method, one must have control of the magnitude of the fundamental component which is also done from the switching angles.

Analysing the output voltage, v_{an}, of a CHB inverter with S bridges, as in Fig. 2, the Fourier coefficients, C_h, can be obtained as:

$$C_h = \frac{4E}{h\pi} \sum_{k=1}^{S} \cos(h\theta_k) \tag{2}$$

According to the Fourier coefficients and knowing that all harmonics are in phase with each other, the time evolution of the output voltage is given by

$$v_{an}(t) = \frac{4E}{\pi} \sum_{h=1}^{\infty} \{ \frac{1}{h} \sum_{k=1}^{S} \cos(h\theta_k) \sin(h\omega t) \} \tag{3}$$

From (2), it can be easily obtained the expression for the peak amplitude of the fundamental component under controlled modulation index; it is given by (4):

$$V_{an1} = \frac{4E}{\pi} \sum_{k=1}^{S} \cos(\theta_k) \tag{4}$$

The expressions that relate the switching angles to a specific objective are obtained from the Fourier series. With five bridges, if it is desired to control the fundamental component and eliminate the first four odd harmonics, the following system of equations is obtained:

$$\begin{cases} \cos(\theta_1) + \cos(\theta_2) + \cos(\theta_3) + \cos(\theta_4) + \cos(\theta_5) = 5m_a \\ \cos(3\theta_1) + \cos(3\theta_2) + \cos(3\theta_3) + \cos(3\theta_4) + \cos(3\theta_5) = 0 \\ \cos(5\theta_1) + \cos(5\theta_2) + \cos(5\theta_3) + \cos(5\theta_4) + \cos(5\theta_5) = 0 \\ \cos(7\theta_1) + \cos(7\theta_2) + \cos(7\theta_3) + \cos(7\theta_4) + \cos(7\theta_5) = 0 \\ \cos(9\theta_1) + \cos(9\theta_2) + \cos(9\theta_3) + \cos(9\theta_4) + \cos(9\theta_5) = 0 \end{cases} \tag{5}$$

subjected to $0 < \theta_1 < \theta_2 < \theta_3 < \theta_4 < \theta_5 < \pi/2$.

For the fundamental component, the amplitude modulation index is defined as:

$$m_a = \frac{\pi}{4E} \frac{V_{an1}}{S} \tag{6}$$

The system of equations is non-linear and can be solved off-line or in real-time. In the first case, the system is solved and the results (switching angles) are stored in memory for use in controlling the various bridges. There are several numerical methods capable of solving the system of equations, [5,6]: Newton's method, method of the resulting polynomials, [4], among others. All of these iterative methods require large computation effort, both at runtime and in memory, which makes it difficult to implement them in real-time on digital platforms (e.g., microcontrollers or digital signal processors). On the other hand, as the number of levels increases (i.e. number of angles to be calculated), the nonlinearity of the system increases significantly, requiring much longer processing time. Thus, the angles are initially calculated for a wide range of modulation indices and stored in tables for later real-time use.

This procedure is extensible to DC sources of different value or variable in time in the various inverters, and the tables must contain all input voltage alternatives and the entire modulation index range. The size of the tables obviously depends on the resolution of the modulation index and the interpolation process defined to obtain the angles associated with intermediate modulation indices.

In the second case, real-time algorithms, several alternative methods are also available to obtain the switching angles: theory of balancing of the voltage-time area of the reference voltage in relation to the output voltage, [7]; by the analytical approximation of the THD expression of the output voltage, [8]. One of the characteristics common to all methods is that there is no control of the amplitude of harmonics not eliminated or not considered for minimization; its value depends on the point of operation and tends to be quite variable.

2.3 THD Minimization

In this work, the method that minimizes THD was selected for analysis and demonstration, [9]. In fact, the method minimizes $(\text{THD})^2$; it is equivalent and simpler and exhibits faster procedures. The THD is given by:

$$THD = \frac{\sqrt{\sum_{h=2}^{\infty} V_h^2}}{V_1} \tag{7}$$

It is difficult to achieve the minimization of THD directly because the numerator of (7) has an infinite number of terms. One solution is to eliminate only a finite number of harmonics. Generally, one eliminates a few low-order harmonics because they contribute more to THD, namely of the current. In a cascade multilevel inverter with S H-bridges, only $(S-1)$ low-order harmonics can be eliminated, which is done in selective harmonic elimination methods, [5].

In [8], through a deductive process, the minimization of $(\text{THD})^2$ value for S bridges is defined and an implicit expression is obtained for an auxiliary variable, ρ, on which all switching angles depend. The procedure, to run in real-time, uses the following two steps:

1. Determine ρ by solving the equation:

$$0 = \sum_{k=1}^{S} \sqrt{1 - \left(\frac{k - 1/2}{S - 1/2}\rho\right)^2} - m_a S \tag{8}$$

2. Determine the switching angles by evaluating

$$\theta_k = \arcsin\left(\frac{k - 1/2}{S - 1/2}\rho\right), k = 1, 2, \ldots, S. \tag{9}$$

From the different possible alternatives it was used the method of Newton due to require a very low number of iterations to determine ρ and a numerically efficient coding thus allowing the operation in real-time.

The factors that determine the speed of convergence of the method are: the initial angle, the evolution of the function (8) and its derivative around the solution. The limits where there is no solution for either m_a or S are easily determined from the analysis of (8): for $S = 3$, m_a must be greater than 0.6; for $S = 5$, m_a must be greater than 0.72. Restriction of the range of m_a as S increases may be a major drawback depending on the type of application.

3 Voltage Range and Distortion

Any inverter must be able to control both the fundamental component of the output voltage and its frequency. Frequency variation is an easy goal to meet; depends on the phase variation of an alternating quantity and is independent of the amplitude variation. Amplitude variation in both static and dynamic terms requires other procedures. According to the foregoing, the limits of the range of the fundamental component of the output voltage are a characteristic of the modulation method and the number of inverter bridges.

3.1 Switching Angles Dynamics

In this work, an inverter with different numbers of H-bridge was simulated. The first step was the validation of the real-time characteristics of the modulation method in the simulation environment using a fundamental frequency of 50 Hz and with $E = 50$ V for three and seven bridges and $E = 40$ V for five bridges. With three, five and seven H-bridges the control algorithm was tested in two conditions: slow and fast variation of the modulation index. For three bridges, m_a varies between 0.67 and 0.98 in 40 ms (slow variation) and 2 ms (fast variation) as shown in Fig. 3. The same conditions were used to test the algorithm with five and seven bridges: amplitude variation from $m_a = 0.73$ to 0.98 in 40 ms (slow variation) and 2 ms (fast variation), and from $m_a = 0.98$ to 0.73 in 2 ms, as shown in Fig. 4, for five bridges, and from $m_a = 0.76$ to 0.98 in 40 ms and 2 ms, and from $m_a = 0.98$ to 0.73 in 2 ms, as shown in Fig. 5, for seven bridges.

The analysis of the three sets of results allows to conclude that the switching angles are updated almost instantaneously after four cycles of the iterative process. The maximum number of iterations depends on the utilized software/hardware platform and is discussed in the implementation and results section.

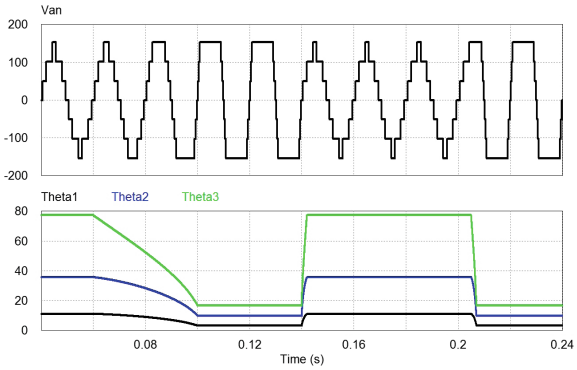

Fig. 3. Output voltage and switching angles for slow and fast changes of the modulation index with three H-bridges. (V_{an}: 100 V/div; $Theta_i$: 20 degrees/div).

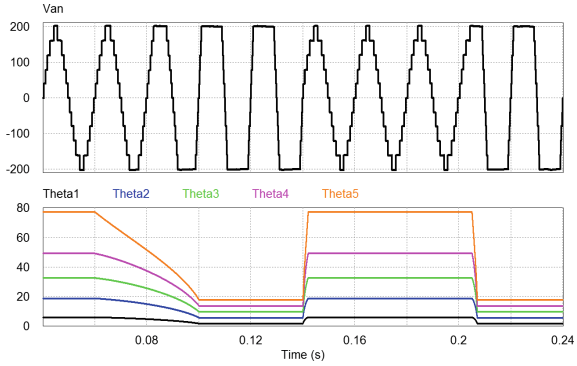

Fig. 4. Output voltage and switching angles for slow and fast changes of the modulation index with five H-bridges. (V_{an}: 100 V/div; $Theta_i$: 20 degrees/div).

A detail of Fig. 4, dynamic variation of the modulation index for five H-bridges, with m_a increasing from 0.73 to 0.98 in 100 ms, is presented in Fig. 6.

The modulation method does not eliminate specific harmonics, but minimizes the voltage THD. Thus, it is important to verify the evolution of low-frequency harmonics, which contribute the most to distorting the output current in loads with inductive characteristics.

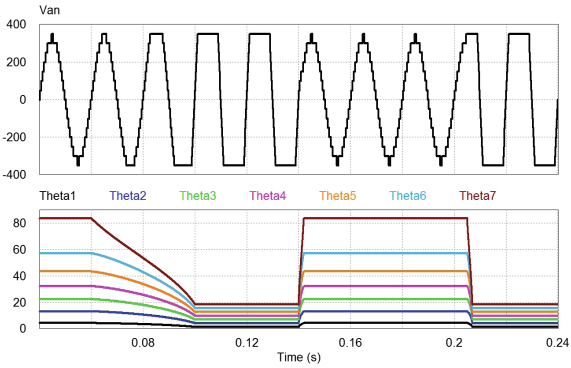

Fig. 5. Output voltage and switching angles for slow and fast changes of the modulation index with seven H-bridges. (V_{an}: 200 V/div; $Theta_i$: 20 degrees/div).

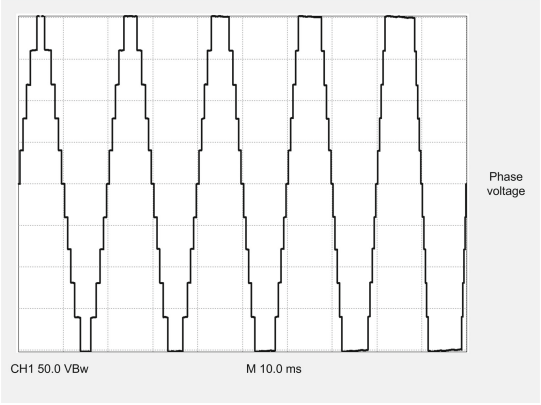

Fig. 6. Increasing modulation index with five bridges (50 V/div; 10 ms/div).

In this subsection it is focused only the five bridge inverter; the other configurations have the same qualitative behaviour and the differences will be discussed later.

Figure 7 shows the evolution of the amplitude of all odd harmonics multiples of 3 up to the 15th, in function of the modulation index; these harmonics are cancelled in a three-phase system. Figure 8 is similar to Fig. 7 but represents only harmonics non-multiples of 3 up to the 19th.

The output voltage THD, with and without harmonics multiples of three, is shown in Fig. 9 and clearly demonstrates the influence of the low-frequency harmonics, mainly the third, fifth and seventh.

The steady-state single-phase voltage is demonstrated in the next figures. For three bridges, it is shown in Fig. 10, for $E = 50$ V, $m_a = 0.75$ and $f = 50$ Hz; also presented is the voltage spectrum, showing the residual low-frequency components characterizing the method; THD is ≈15%. The topology considering

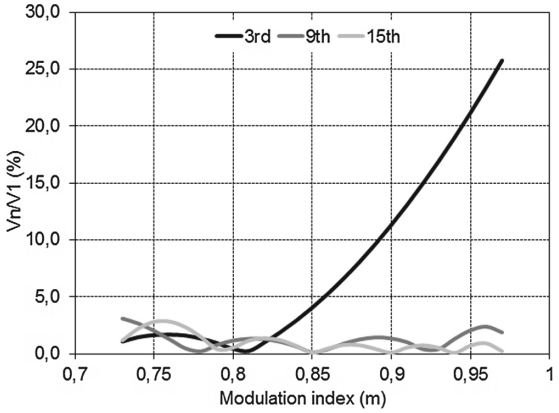

Fig. 7. Odd harmonics multiples of three for five H-bridges.

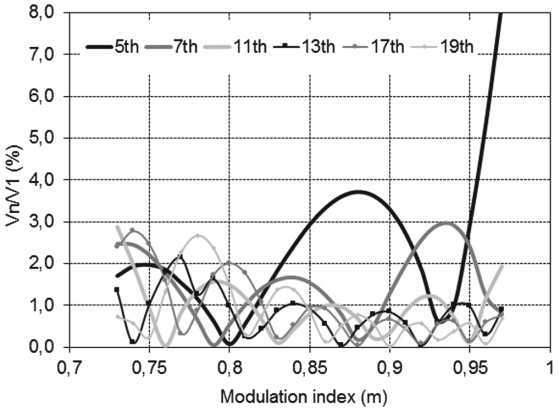

Fig. 8. Odd harmonics non-multiples of three for five H-bridges.

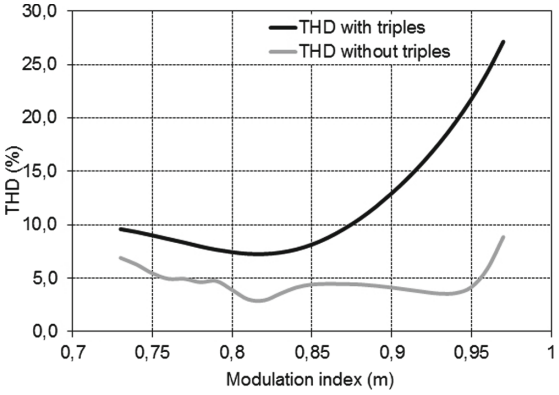

Fig. 9. THD of the output voltage for five H-bridges, with and without the triple harmonics.

five bridges was also simulated and the steady-state single-phase voltage is shown in Fig. 11, now with $E = 40$ V, $m_a = 0.8$ and $f = 50$ Hz. THD is ≈7.5%, much smaller than the one with three bridges. Finally, the seven bridges inverter is shown in Fig. 12, now with $E = 50$ V, $m_a = 0.83$ and $f = 50$ Hz; the THD is ≈6%, the smallest one. More comparative results, for the whole range of modulation index, will be shown later, in Figs. 19 and 20.

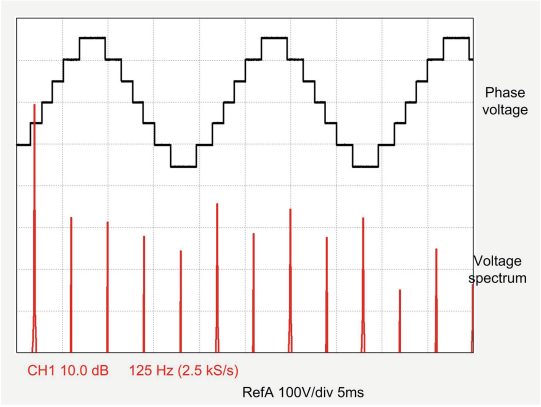

Fig. 10. Inverter output voltage with three H-bridges (100 V/div; 5 ms/div) and harmonic spectrum (10 dB/div; 125 Hz/div).

The method works well for a restricted range of modulation index values, not converging for other (smaller) values of m_a. On the other hand, in the upper range of modulation index values (e.g. greater than 0.87 for THD <10%, see Fig. 9) the THD value is quite high which may make it not feasible to use. It is therefore necessary to evaluate the range of operation of the inverter in terms of the amplitude of the fundamental component knowing that it decreases as the number of bridges constituting it increases.

4 Implementation and Results

A FGPA board, which incorporates a soft processor and peripheral analogue and digital I/O, was used to implement the complete process of calculating the switching angles for the inverters and transferring them to dedicated timers. The prototype of the developed CHB inverter has five bridges, each powered by an isolated DC voltage source of 40 V (experiments with three bridges were done using a DC voltage level of 50 V). The presented experimental results are focused on the characterization of the modulation method for a different number of levels. The features to be analysed are, as mentioned above, low order harmonics, THD and real-time dynamics.

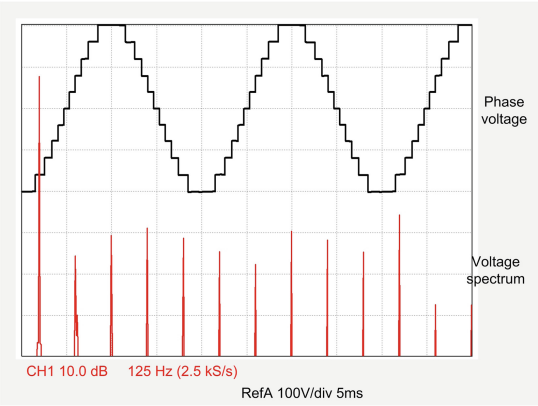

Fig. 11. Inverter output voltage with five H-bridges(100 V/div; 5 ms/div) and harmonic spectrum (10 dB/div; 125 Hz/div).

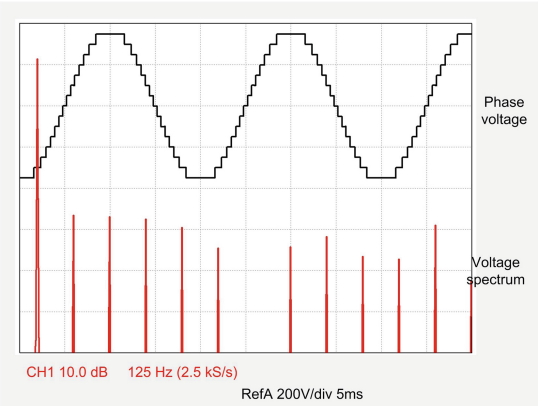

Fig. 12. Inverter output voltage with seven H-bridges (200 V/div; 5 ms/div) and harmonic spectrum (10 dB/div; 125 Hz/div).

4.1 Low-Frequency Harmonics and THD

The amplitude of the low-frequency harmonics, which is variable as a function of the modulation index, is shown in Figs. 13 and 14. The comparison with Figs. 7 and 8 (in the simulation environment) demonstrates the correct implementation of the command method.

The total harmonic distortion, shown in Fig. 15, has an absolute minimum value for small modulation indices and, as already obtained in simulation, increases rapidly for high modulation indices. The result has a good agreement with that obtained by simulation in Fig. 9.

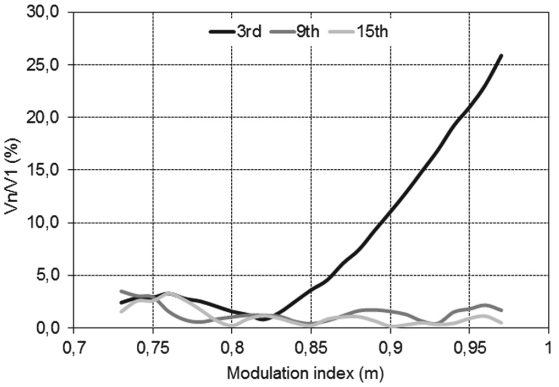

Fig. 13. Odd harmonics multiples of three for five H-bridges (experimental).

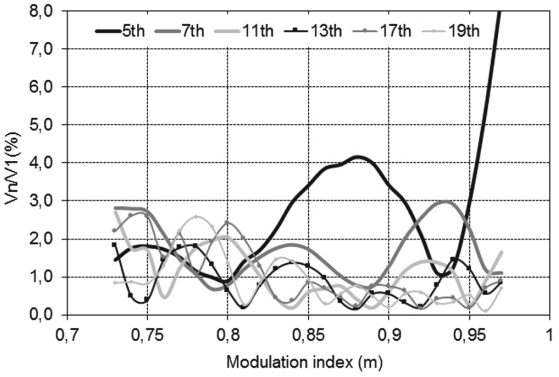

Fig. 14. Odd harmonics non-multiples of three for five H-bridges (experimental).

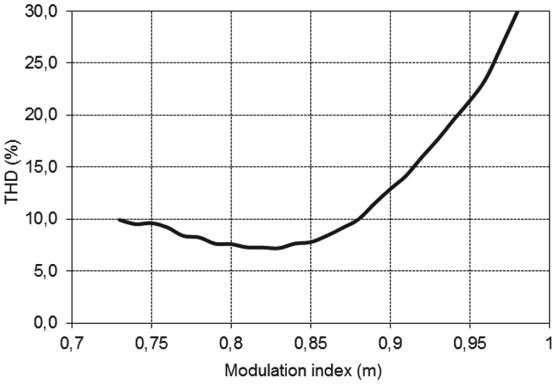

Fig. 15. THD of the output voltage for five H-bridges (experimental).

4.2 Voltage Dynamics

As an illustration of the variation of the modulation index, Fig. 16 shows the evolution of the output voltage when m_a changes from 0.73 to 0.98 in 100 ms.

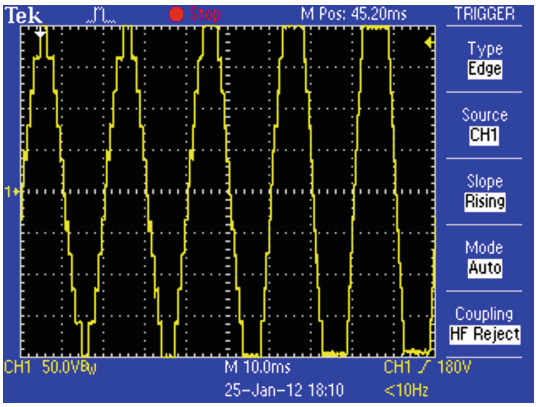

Fig. 16. Experimental dynamic variation of the modulation index.

The steady-state output voltage of the three-bridge inverter is shown in Fig. 17, using the same conditions as in Fig. (V_{dc}, m_a and f) and one can verify a high degree of similarity between the experimental and simulated results.

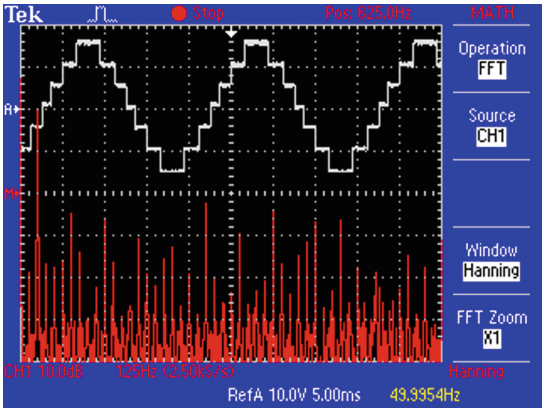

Fig. 17. Experimental output voltage and harmonic spectrum for three bridges.

In Fig. 18, for five bridges, is shown the steady-state AC voltage using $E = 40$ V, $m_a = 0.8$, with $f = 50$ Hz. It is also presented the harmonic spectrum of the voltage.

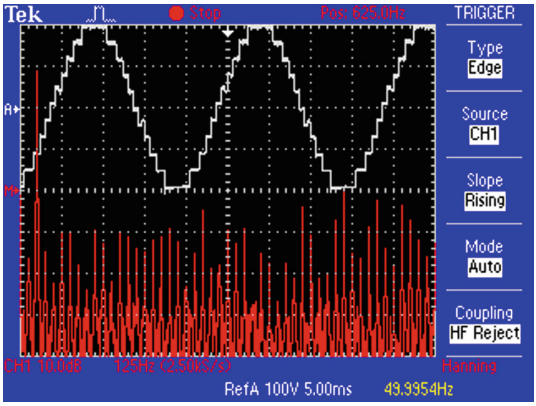

Fig. 18. Experimental output voltage and harmonic spectrum for five bridges.

As expected from the simulations, the spectrum is a widespread one, showing low-frequency components. The results in Figs. 17 and 18 compare with the ones in Figs. 10 and 11, respectively, and they are quite similar.

4.3 Discussion

For a global characterization, the method was simulated with three, five and seven bridges and was experimentally validated with three and five bridges. With respect to the fundamental component, the range of variation of m_a is reduced with the increase of the number of bridges. It is also found that the limits of the range of modulation indices in which a relatively small THD occurs are reduced as the number of bridges increases.

In any configuration, the THD is high for high modulation indices. In this region, however, the voltage waveform is close to a square wave which is not desirable in any application. These conclusions are documented in Figs. 19 and 20. Generally, there is a contradiction with the high number of degrees of freedom in the inverter control (the switching angles).

There are other methods also with real-time capability that do not minimize THD, as the one developed in [10].

When compared to the expected dynamics at the output of a current controller, the analysed method provides sufficiently rapid changes in amplitude and phase although within a relatively small range. It thus enables effective control of a power converter provided that the variations occur in the vicinity of a given reference to the voltage output. Two classes of applications can therefore be distinguished: those relating to drives, where the frequency variation implies a wide variation of modulation indices, and those relating to applications where the converter is connected to the electric network, where the method operates with good characteristics.

The concept that supports the method is applicable to any number of bridges but the available range of variation of the fundamental component is decreasing.

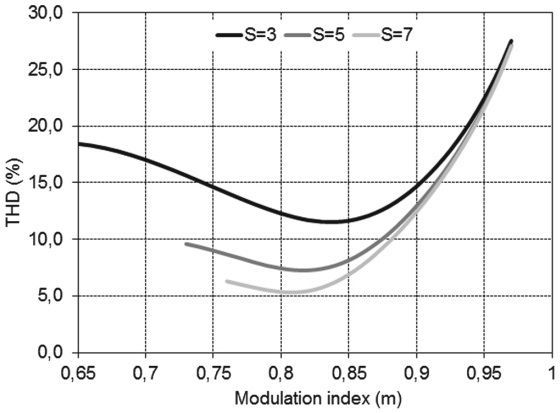

Fig. 19. THD of the output voltage for three, five and seven H-bridges (simulation).

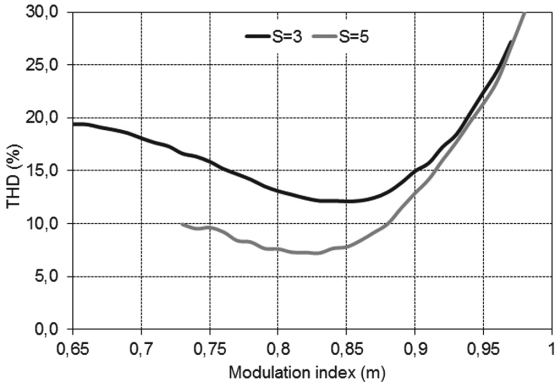

Fig. 20. THD of the output voltage for 3 and five H-bridges (experimental).

The question arises as to what is the number of bridges of an inverter from which it is no longer possible to apply it in converters connected to the electric grid.

5 Conclusion

The method described and implemented to determine the switching angles of each individual H-bridge requires a reduced number of iterations. Therefore, it can be easily implemented in a real-time control board, such as uP/DSP/FPGA. The experimental analysis of the characteristics of the method allows to conclude that it is compatible with the interface of power electronic converters with the electric network. The method can be applied to a larger number of H-bridges (7, 9, ...) with similar characteristics.

Acknowledgments. This work was financially supported by: Project POCI-01-0145-FEDER-006933/SYSTEC - Research Center for Systems and Technologies funded by FEDER funds through COMPETE 2020 and by national funds through the FCT/MEC, and co-funded by FEDER, in the scope of the PT2020 Partnership Agreement. Abel A. Ferreira gratefully acknowledges the financial support from the People Programme (Marie Curie Actions) of the European Union's Seventh Framework Programme FP7/2007-2013/ (Grant Agreement no. 317221), project title MEDOW.

References

1. Rodriguez, J., et al.: Multilevel converters: an enabling technology for high-power applications. Proc. IEEE **97**(11), 1786–1817 (2009)
2. Malinowski, M., Gopakumar, K., Rodriguez, J., Pérez, M.A.: A survey on cascaded multilevel inverters. IEEE Trans. Ind. Electron. **57**(7), 2197–2206 (2010)
3. Holmes, D.G., Lipo, T.: Pulse Width Modulation for Power Converters. Wiley/IEEE Press, New York (2003)
4. Chiasson, J.N., Tolbert, L.M., McKenzie, K.J., Du, Z.: A unified approach to solving the harmonic elimination equations in multilevel converters. IEEE Trans. Power Electron. **19**(2), 478–490 (2004)
5. Dahidah, M.S., Konstantinou, G., Agelidis, V.G.: A review of multilevel selective harmonic elimination PWM: formulations, solving algorithms, implementation and applications. IEEE Trans. Ind. Electron. **30**(8), 4091–4116 (2015)
6. Hong, D., Bai, S., Lukic, S.M.: Closed-form expressions for minimizing total harmonic distortion in three-phase multilevel converters. IEEE Trans. Power Electron. **29**(10), 5229–5241 (2014)
7. Rathore, A.K., Holtz, J., Boller, T.: Generalized optimal pulsewidth modulation of multilevel inverters for low-switching-frequency control of medium-voltage high-power industrial AC drives. IEEE Trans. Ind. Electron. **60**(10), 4215–4224 (2013)
8. Liu, Y., Hong, H., Huang, A.Q.: Real-time calculation of switching angles minimizing THD for multilevel inverters with step modulation. IEEE Trans. Ind. Electron. **56**(2), 285–293 (2009)
9. Faria, J., Martins, A.: Analysis and characterization of a square-wave modulation method for single-phase cascaded H-bridge multilevel inverters. In: Proceedings of the International Conference on Renewable Energies and Power Quality (ICREPQ 2012), 28–30 March 2012, Santiago de Compostela, Spain (2012)
10. Kang, D.-W., Kim, H.-V., Kim, T.-J., Hyun, D.-S.: A simple method for acquiring the conducting angle in a multilevel cascaded inverter using step pulse waves. IEE Proc.-Electr. Power Appl. **152**(1), 103–111 (2005)